

LETTER TO THE EDITOR

Evolution of tumor microenvironment in colorectal liver metastases under treatment stress

Dear editor,

The tumor microenvironment (TME) heavily impacts disease biology and may influence responses to systemic treatments, and thereby, affects patients' prognosis. In our previous study, we found that immune features could predict prognosis and guide the therapy choices for stage I-III colon cancer [1,2]. Increasing evidence shows that therapy-induced TME changes can promote tumor progression, metastasis, and the development of resistance [3,4]. However, the TME dynamics in colorectal liver metastases (CRLM) under treatment are still incompletely clear.

In this study, we surveyed the evolution of the TME under treatment stress from 15 CRLM patients via RNA sequencing (RNA-seq), T-cell receptor (TCR) sequencing (TCR-seq), immunohistochemical (IHC) staining and immunofluorescence (Supplementary Materials and Methods) (Supplementary Figure S1A, and Supplementary Table S1). During treatment, the fraction of epithelial tumor cells of regressive tumors (partial response [PR]) decreased significantly, whereas it increased in stable and progressive tumors (SD and PD) (Supplementary Figure S1B-D). Consensus molecular subtypes, which is one of the most robust colorectal cancer classifications, changed dramatically during treatment (Supplementary Figure S1E).

Comparison of treatment-naïve patients with response (PR) and non-response (SD or PD) showed that along with the upregulation of interferon response, the expression of immune checkpoint-related genes also increased (Supplementary Figure S2A-C). Immune-related genes were significantly enriched in sensitive tumors after treatment whereas progressive tumors contained highly expressed

genes involved in fatty acid, amino acid metabolism and cholesterol homeostasis (Supplementary Figure S2D-F). Analysis of matched pre- and post-therapy samples revealed that upregulated genes in responders during therapy were immune-related, whereas these genes were downregulated in non-responders (Supplementary Figure S2G-I). Gene Set Enrichment Analysis (GSEA) revealed that the response of interferon and inflammation was upregulated during treatment in responders, but was downregulated in non-responders (Supplementary Figure S2J).

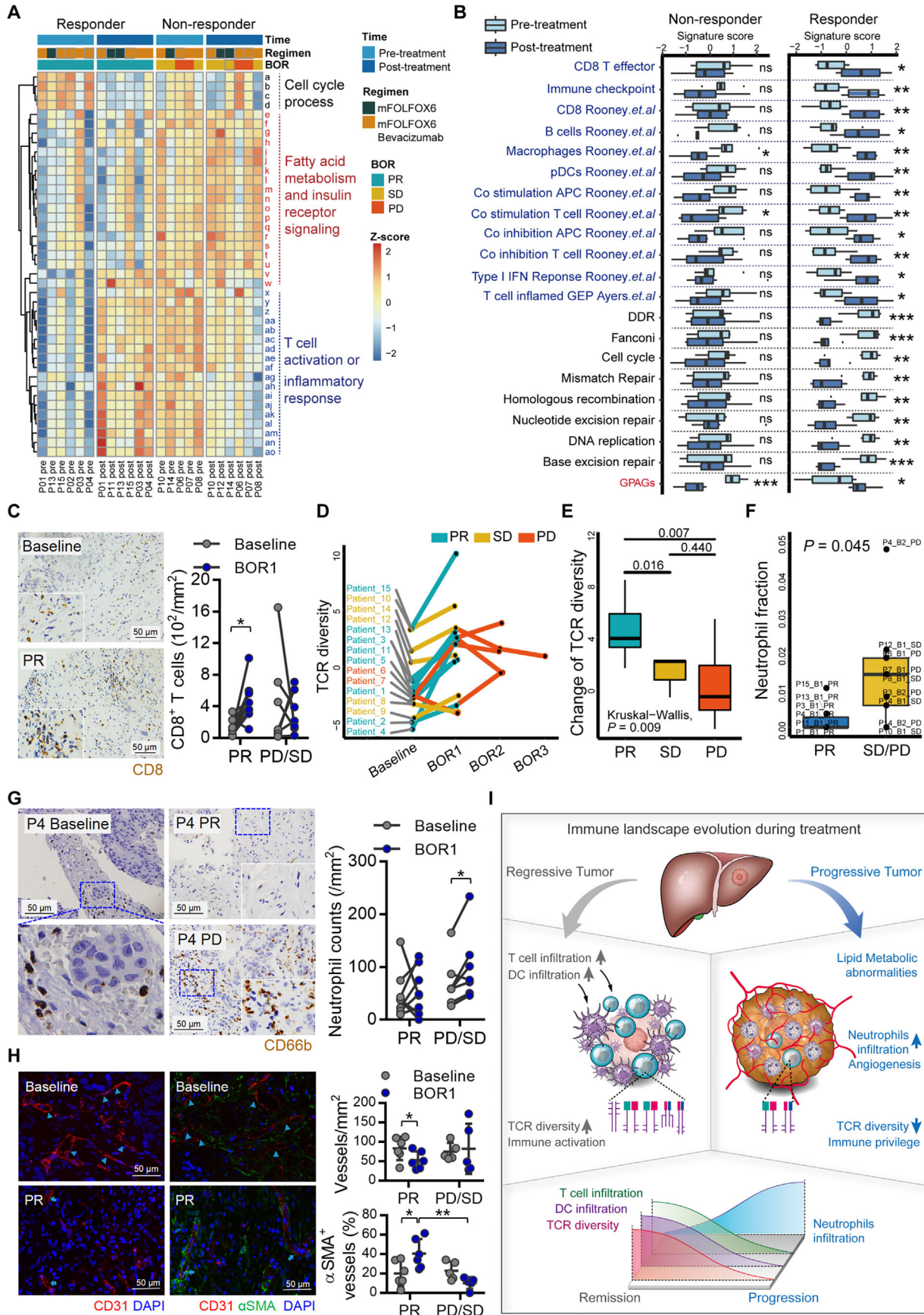
Single sample gene set enrichment analysis (ssGSEA) [5] indicated that immune infiltration in regressive tumors was increased, whereas tumor cell cycle and DNA metabolic processes were decreased during therapy (Figure 1A, and Supplementary Figure S3A-B). Conversely, immune-activation relevant signature scores decreased, whereas tumor cell-cycle processes fluctuated in non-responders (Supplementary Figure S3A, C). As shown in Figure 1B, with the application of gene sets [6], immune infiltration in responsive tumors after treatment was higher than before treatment. Dendritic cells, antigen-presenting cells and T cells were upregulated in shrinking tumors but not changed significantly in progressive metastatic tumors. The good-prognosis angiogenesis genes (GPAGs) score [7], which may reflect vessel normalization, was increased after treatment in responders, whereas it was decreased in non-responders. Overall, the RNA-based immune signatures from tumor tissue suggested that therapy remodeled TME, which correlated with treatment benefits.

IHC analysis showed that the densities of CD8⁺ T cells in tumors were significantly increased after treatment in responders ($P = 0.011$; Figure 1C). However, in non-responders, CD8⁺ T-cell densities were slightly but not significantly decreased. TCR-seq indicated that four TCR diversity indexes of tumors were significantly increased in responders during treatment but were unchanged in non-responders (Supplementary Figure S4A-C). TCR diversity scores which were defined according to the sum of four

Abbreviations: BOR, best overall response; CRLM, colorectal cancer liver metastases; GPAGs, good-prognosis angiogenesis genes.; GSEA, gene set enrichment analysis; IHC, immunohistochemical; PD, progressive disease; PR, partial response; RNA-seq, RNA sequencing; SD, stable disease; ssGSEA, single sample gene set enrichment analysis; TCR, T-cell receptor; TCR-seq, TCR sequencing; TME, Tumor microenvironment

This is an open access article under the terms of the [Creative Commons Attribution-NonCommercial-NoDerivs](https://creativecommons.org/licenses/by-nc-nd/4.0/) License, which permits use and distribution in any medium, provided the original work is properly cited, the use is non-commercial and no modifications or adaptations are made.

© 2022 The Authors. *Cancer Communications* published by John Wiley & Sons Australia, Ltd. on behalf of Sun Yat-sen University Cancer Center.



diversity indexes, increased as the tumors shrank, and decreased as the tumors progressed (Figure 1D–E, and Supplementary Figure S4D). These findings confirmed responsive tumors had immune remodeling, including elevated T-cell infiltration and activation, increased TCR diversity, as well as enhanced antigen presentation.

Deconvoluted by the CIBERSORT algorithm [8], the fraction of neutrophils and monocytes were significantly more numerous in progressive tumors (Figure 1F, and Supplementary Figure S5A). IHC staining confirmed that neutrophil density was significantly increased after treatment in non-responders ($P = 0.032$; Figure 1G), whereas there were no changes in tumor-associated macrophage (Supplementary Figure S5B). Meanwhile, we deconvoluted bulk RNA-seq profiles of the TCGA Pan-Cancer dataset and validated the poor outcome of patients with high neutrophil infiltration (Supplementary Figure S5C). Remarkably, correlation analysis of the TCGA Pan-Cancer data revealed a significant positive correlation between neutrophils and fatty acid metabolism, and a negative correlation between neutrophils and T-cell immunity (Supplementary Figure S5D–E). These results suggested a major role of fatty acid metabolism–neutrophil crosstalk in treatment resistance.

Transcriptome analyses showed that VEGF-A inhibition increased intra-tumor T-cell abundance and upregulated the expression of immune checkpoint-relevant genes

after treatment (Supplementary Figure S6A). GSEA and ssGSEA analysis indicated that tumors treated with bevacizumab plus chemotherapy significantly upregulated the interferon response, TNF- α signaling pathways and T-cell receptor signaling pathway (Supplementary Figure S6B–C), suggesting that chemotherapy with bevacizumab promoted tumor T-cell infiltration and activation. Analysis of responders who had received chemotherapy plus bevacizumab revealed that VEGF-A inhibition activated T cells, facilitated leukocyte migration, and upregulated inflammatory responses (Supplementary Figure S6D–E). Responders had decreased vessel density ($P = 0.043$) and increased proportion of normalized vessels (α -SMA⁺ vessels; $P = 0.023$) after treatment (Figure 1H). The HIF1 α expression in responders after treatment was lower than before treatment ($P = 0.023$) and in non-responders after treatment ($P = 0.016$; Supplementary Figure S6F). These results suggested that the infiltration of T-cell was associated with tumor vasculature normalization.

In conclusion, under treatment stress, the TME was remodeled to promote T-cell immunity and vasculature normalization in responders, whereas in non-responders, both lipid metabolism in the tumor and neutrophil infiltration in the TME increased (Figure 1I). Based on the dynamic analysis of clinical samples, our findings are closer to the clinical settings, contributing to the

FIGURE 1 Tumor microenvironment evolution in colorectal liver metastases during treatment. (A) Heatmap-depicted metabolism activity and immune signatures. The related signatures were obtained from Gene Ontology (GO) and Kyoto Encyclopedia of Genes and Genomes (KEGG) pathway from the MSigDB database of Broad Institute. Then, the gene set was scored by the ssGSEA method and statistically analyzed. (B) Changes in T cell activation and cell cycle-related signature scores, and GPAGs of non-responders and responders from pre-treatment to post-treatment. (C) Representative IHC images and density quantification of CD8⁺ T cells in the tumor before and after treatment. Total magnification, $\times 400/\times 800$. (D) Changes in the TCR diversity score in patients. (E) Changes of TCR diversity with various treatment outcomes. (F) Neutrophil differences from responders and non-responders after treatment. (G) Representative IHC images and density quantification showing neutrophil infiltration during treatment. Total magnification, $\times 400/\times 950/\times 1800$. (H) Representative vascular morphology images (triangle and arrows). Vessel density and α -SMA⁺ vessels change during treatment. (I) Schematic of the TME dynamics during treatment. Bars show the Mean \pm SD. P value is based on a two-tailed paired Student's t -test (B, C, G and H), and a two-tailed Student's t -test (H). * $P < 0.05$, ** $P < 0.01$, *** $P < 0.001$. Abbreviations: (A) BOR: best overall response; PR: partial response; SD: stable disease; PD: progressive disease; a: KEGG DNA replication; b: GO DNA metabolic process; c: GO Cell cycle; d: GO Cell cycle process; e: GO Glycerophospholipid metabolic process; f: GO Regulation of insulin like growth factor receptor signaling pathway; g: GO Brown fat cell differentiation; h: GO Positive regulation of lipid storage; i: KEGG Lysine degradation; j: GO Regulation of glucose metabolic process; k: GO Positive regulation of triglyceride metabolic process; l: GO Tetrahydrofolate metabolic process; m: KEGG Fatty acid metabolism; n: GO Fatty acid metabolic process; o: GO Positive regulation of steroid metabolic process; p: GO Positive regulation of fatty acid metabolic process; q: GO Regulation of fatty acid biosynthetic process; r: GO Positive regulation of cellular response to insulin stimulus; s: GO Hemoglobin metabolic process; t: GO Regulation of cellular response to insulin stimulus; u: GO Regulation of insulin receptor signaling pathway; v: GO Amino sugar metabolic process; w: GO Unsaturated fatty acid biosynthetic process; x: GO Antigen processing and presentation; y: GO Cellular response to lipoprotein particle stimulus; z: GO Leukocyte migration; aa: GO Endocytosis; ab: GO Positive regulation of response to stimulus; ac: GO Positive regulation of inflammatory response; ad: GO Regulation of activated T cell proliferation; ae: KEGG JAK STAT signaling pathway; af: GO Adaptive immune response; ag: GO Cytokine metabolic process; ah: KEGG Lysosome; ai: GO Positive regulation of mast cell activation; aj: KEGG Chemokine signaling pathway; ak: GO Leukocyte proliferation; al: GO Regulation of alpha beta T cell differentiation; am: GO Negative regulation of nitric oxide metabolic process; an: KEGG T cell receptor signaling pathway; ao: GO Regulation of B cell proliferation; P: patient; pre: pre-treatment; post: post-treatment. (B) GPAGs: good-prognosis angiogenesis genes; (D) TCR: T-cell receptor; (F) B1, the first best overall response; B2, the second best overall response; (I) DC: dendritic cell

improvement of therapy, and providing valuable clues for further exploration into the relationship between resistance, lipid metabolism and the TME.

DECLARATIONS

ACKNOWLEDGMENTS

Not applicable.

FUNDING

This work was supported by grants from the National Natural Science Foundation of China (81772580), Natural Science Foundation of Guangdong Province, China (2021A1515011705), and the Clinical Research Startup Program of Southern Medical University by High-level University Construction Funding of Guangdong Provincial Department of Education (LC2016ZD014).

COMPETING INTERESTS

The authors declare that they have no competing interests.

ETHICS APPROVAL AND CONSENT TO PARTICIPATE

Patients' samples were collected and analyzed after informed consents were obtained and approved by the ethics committee (NFEC-2017-206) of Nanfang Hospital, Southern Medical University (Guangzhou, China).

AUTHORS' CONTRIBUTIONS



Study design: MS and WJL; Clinical data acquisition and sample annotation: NH, XXR, CLW, ZZW, JG and JW; Bioinformatics analysis and data visualization: DQZ, XY, YQW, Jin Li, Jing Li, and QL; Performance and analysis of immunohistochemistry and immunofluorescence: GJH and STZ; Statistical analysis: NH, DQZ, and XY; Drafting and critical revision of the manuscript: MS, WJL, NH, DQZ, JPB, and YLL. All authors have read and approved the final manuscript.


AVAILABILITY OF DATA AND MATERIALS

The datasets generated and analyzed during the current study are available in the Gene Expression Omnibus (GEO; <https://www.ncbi.nlm.nih.gov/geo/query/acc.cgi?acc=GSE136114>; accession number: GES136114).

CONSENT FOR PUBLICATION

Not applicable.

Na Huang¹
Dongqiang Zeng¹ 
Xiaoxiang Rong¹ 
Chunlin Wang¹
Zhenzhen Wu¹
Jian Guo¹

Yuqi Wang²
Jin Li²
Jing Li²
Jiao Wang¹
Siting Zheng¹
Genjie Huang¹
Jianping Bin³
Yulin Liao³
Qian Li²
Xin Yi²
Wangjun Liao¹ 
Min Shi¹ 

¹ Department of Oncology, Nanfang Hospital, Southern Medical University, Guangzhou, Guangdong 510515, P. R. China

² Department of Research and Development, GenePlus-Beijing, Beijing 102206, P. R. China

³ Department of Cardiology, Nanfang Hospital, Southern Medical University, Guangzhou, Guangdong 510515, P. R. China

Correspondence

Min Shi, Department of Oncology, Nanfang Hospital, Southern Medical University, 1838 North Guangzhou Avenue, Guangzhou 510515, Guangdong, P. R. China.

Email: nfyshimin@163.com

Wangjun Liao, Department of Oncology, Nanfang Hospital, Southern Medical University, 1838 North Guangzhou Avenue, Guangzhou 510515, Guangdong, P. R. China.

Email: nfyyliaowj@163.com

Xin Yi, Department of Research and Development, GenePlus-Beijing, Zhongguancun Life Science Park, Changping District, Beijing 102206, P. R. China.

Email: yix@geneplus.org.cn

Na Huang, Dongqiang Zeng and Xiaoxiang Rong contributed equally to this work.

ORCID

Dongqiang Zeng  <https://orcid.org/0000-0001-9724-8325>

Xiaoxiang Rong  <https://orcid.org/0000-0002-5058-2067>

Wangjun Liao  <https://orcid.org/0000-0002-1364-8442>

Min Shi  <https://orcid.org/0000-0003-0113-4089>

REFERENCES

1. Zhou R, Zhang J, Zeng D, Sun H, Rong X, Shi M, et al. Immune cell infiltration as a biomarker for the diagnosis and prognosis of stage I-III colon cancer. *Cancer Immunol Immunother.* 2019;68:433-42.
2. Zhou R, Zeng D, Zhang J, Sun H, Wu J, Li N, et al. A robust panel based on tumour microenvironment genes for

- prognostic prediction and tailoring therapies in stage I-III colon cancer. *EBioMedicine*. 2019;42:420-30.
3. Shaked Y. Balancing efficacy of and host immune responses to cancer therapy: the yin and yang effects. *Nat Rev Clin Oncol*. 2016;13:611-26.
 4. Woolston A, Khan K, Spain G, Barber LJ, Griffiths B, Gonzalez-Exposito R, et al. Genomic and transcriptomic determinants of therapy resistance and immune landscape evolution during anti-EGFR treatment in colorectal cancer. *Cancer Cell*. 2019;36:35-50.
 5. Hänzelmann S, Castelo R, Guinney J. GSVA: gene set variation analysis for microarray and RNA-seq data. *BMC Bioinformatics*. 2013;14:7.
 6. Zeng D, Ye Z, Shen R, Yu G, Wu J, Xiong Y, et al. IOBR: Multi-Omics Immuno-Oncology Biological Research to Decode Tumor Microenvironment and Signatures. *Front Immunol*. 2021;12:687975.
 7. Tian L, Goldstein A, Wang H, Ching LH, Sun KI, Welte T, et al. Mutual regulation of tumour vessel normalization and immunostimulatory reprogramming. *Nature*. 2017;544:250-4.
 8. Newman AM, Liu CL, Green MR, Gentles AJ, Feng W, Xu Y, et al. Robust enumeration of cell subsets from tissue expression profiles. *Nat Methods*. 2015;12:453-7.

SUPPORTING INFORMATION

Additional supporting information may be found in the online version of the article at the publisher's website.